A VLASOV-MAXWELL SOLVER TO STUDY MICROBUNCHING INSTABILITY IN THE FERMI@ELETTRA FIRST BUNCH COMPRESSOR SYSTEM

G. Bassi, University of Liverpool and Cockcroft Institute, Liverpool, UK *

J. A. Ellison, K. Heinemann, University of New Mexico, Albuquerque, USA †

INTRODUCTION

Microbunching can cause an instability which degrades beam quality. This is a major concern for free electron lasers where very bright electron beams are required. A basic theoretical framework for understanding this instability is the 3D Vlasov-Maxwell system. However, the numerical integration of this system is computationally too intensive at the moment. As a result, investigations to date have been done using very simplified analytical models or numerical solvers based on simple 1D models [1-6]. We have developed an accurate and reliable 2D Vlasov-Maxwell solver which we believe improves existing codes. Our solver has been successfully tested against the Zeuthen benchmark bunch compressors. For more details see [7-8] and references therein. In the present contribution we apply our self-consistent, parallel solver to study the microbunching instability in the first bunch compressor system of FERMI@ELETTRA. This system was proposed as a benchmark for testing codes at the September'07 microbunching workshop in Trieste[1].

FERMI@ELETTRA BUNCH COMPRESSOR STUDIES

The complete layout and parameters of the proposed benchmark system are shown in Fig. 1. The system consists of a 4 dipole chicane between rf cavities and quadrupoles. In this contribution we limit our study to the chicane. A complete study is on our agenda. A standard approach to study the microbunching instability consists in calculating a gain factor for a given initial modulation wavenumber k_0 [1-3]. The gain factor is defined as $\mid b(k_f, s_f)/b(k_0, 0) \mid$, where $b(k, s) = \int dz \exp(-ikz)\mu(z, s)$ and $k_f = k_0/(1 + uR_{56}(s_f))$ for a given initial wavelength of $\lambda = 2\pi/k_o$. Here $s_f = 8$m is s at the exit of the chicane and $\mu = \mu(z, s)$ is the longitudinal charge density. The compressor factor of the chicane is $C = 1/((1 + uR_{56}(s_f)) = 3.545$. In Fig. 2 (top left) we compare an analytical formula for the gain factor given in [1], Eq. (38), with the gain factor calculated numerically with our solver. The formula from [1] takes into account only coherent synchrotron radiation (CSR) effects whereas our Vlasov-Maxwell approach automatically includes the effects of CSR and space

charge. Both analytical and numerical gain factors for $\lambda \geq 300\mu$m are close to 1 indicating little or no amplification of the initial modulation. In our studies the initial distribution is assumed to be of the form $f(z, p_z)g(x, p_x)$ where z, x, p_z, p_x are standard machine coordinates. Here g is Gaussian and $f(z, p_z) = \mu(z)\rho_c(z, p_z)$, where μ is a flattop distribution modulated by a perturbation with wavelength λ and a small amplitude A. Specifically, $\mu(z) = [1 + A\cos(2\pi z/\lambda)][\tanh((z+a)/b) - \tanh((z-a)/b)]/4a$ and $\rho_c(z, p_z)$ has the form $\exp[-(p_z - uz)/2\sigma_u]/\sqrt{2\pi\sigma_u}$. Here $a = 0.00118$, $b = 0.00015$ and $A = 0.05$. The uncorrelated energy spread $\sigma_E = 2KeV$ gives $\sigma_u = \sigma_E/E_r = 8.6 \times 10^{-6}$ (recall $p_z = (E - E_r)/E_r$). We calculated the gain factor for an initial modulation of wavelength λ=300, 400, 500 and 600μm. The number of particles used in the simulations is N=2×10^7 and the number of Fourier coefficients used in the estimation of the 2D charge/current density runs from 30×30 for $\lambda = 600\mu$m to 60×60 for $\lambda = 300\mu$m [7-8].

In Fig. 2 (top right) we show the initial charge density for $\lambda = 300\mu$m. The effect of the modulation on the longitudinal force (mean power) and on the transverse emittance is very small for all four λ values. This is shown for $\lambda = 300\mu$m in Fig. 2 (bottom). In Fig. 3 we show the charge density in normalized coordinates at s=8m for $\lambda = 300\mu$m (left) and $\lambda = 600\mu$m (right), and they differ very little from the initial density (see Fig. 2 also). In Fig. 4 (left) we show the same for no initial modulation (A=0). In Fig. 4 (right) we show the longitudinal component of the electric field $\mathbf{E} \cdot \mathbf{t}$ at s=8m for no initial modulation. In Fig. 5 we show the same for $\lambda = 300\mu$m (left) and $\lambda = 600\mu$m (right). Fig. 5 (left) shows a structure with 7 peaks in the range $-0.5 \leq z_n \leq 0.5$ and modulation wavelength of $\approx 300/C\mu$m. The extent of the modulation is 0.0015+0.0028. Fig. 5 (right) shows a structure with 4 peaks in the same range of z_n with a modulation wavelength of $\approx 600/C\mu$m and magnitude 0.005+0.0015. Therefore the ratio of the two ranges is 2.15 showing a bigger amplification of the modulation in $\mathbf{E} \cdot \mathbf{t}$ at $\lambda = 300\mu$m. Comparing Fig. 4 (right) and Fig. 5 we conclude that at s=8m there is an amplification of modulations in $\mathbf{E} \cdot \mathbf{t}$ at the wavelength λ/C while there is no such effect in the charge density. A possible interpretation is that the longitudinal component of the electric field $\mathbf{E} \cdot \mathbf{t}$ has not been amplified enough to dynamically act back on the charge density and create a detrimental effect.

Studies are in progress to understand this effect and to
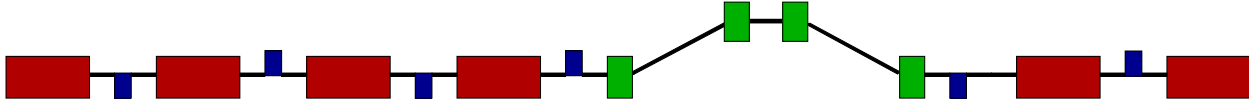

Figure 1: Proposed layout of FERMI@ELETTRA first bunch compressor system. Accelerating rf cavities in red, quadrupole magnets in blue, drift sections in black and dipoles in green. Chicane parameters and beam parameters at first dipole: energy reference particle E_r=233MeV, peak current I=120A, bunch charge Q=1nC, normalize transverse emittance $\gamma\epsilon_0 = 1\mu$m, alpha function α_0=0, beta function β_0=10, linear energy chirp u=-27.5 1/m, uncorrelated energy spread σ_E=2KeV, momentum compaction R_{56}=0.0025m, radius of curvature ρ_0=7.38m, magnetic length L_b=0.5m, distance first-second and third-fourth bend L_1=2.5m, distance second-third bend L_2=1m.
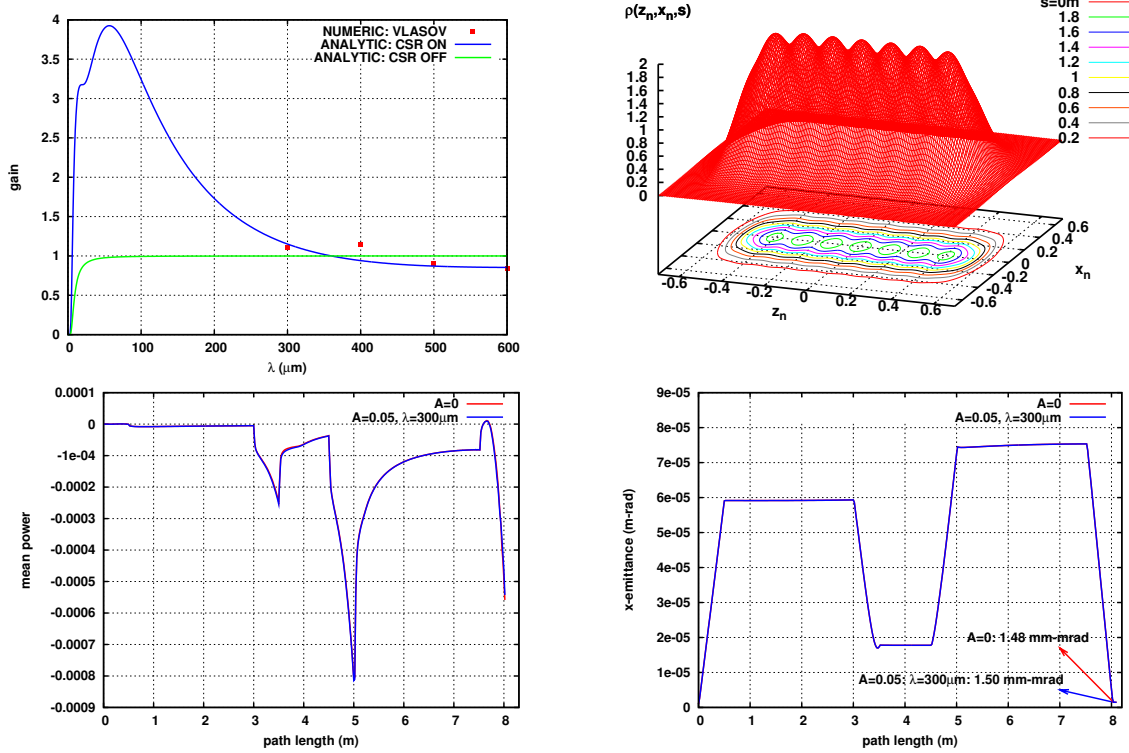

Figure 2: Top left: gain factor from analytical formula in [1] (blue and green curve) and from our Vlasov solver (red square). Top right: initial charge density in normalized coordinates. Bottom left: mean power vs. s with no initial modulation (A=0) (red curve) and with A=0.05, $\lambda = 300\mu$m (blue curve). Bottom right: same as bottom left for the x-emittance.

investigate wavelengths shorter than $\lambda = 300\mu$m and different amplitudes A. Preliminary results at $\lambda = 200\mu$m show an instability in the charge density developing in the second magnet. We are checking to see if this is a numerical artifact.

The major road block to our study of shorter wavelengths is increased storage and computational cost needed. We are working on improving the efficiency of the solver by (1) implementing parallel I/O, (2) replacing our pseudorandom generator of the initial density by a quasirandom generator (e.g., Sobol), see [9], (3) improving the field calculation and (4) replacing the truncated Fourier series density estimator by a kernel smoother.

ACKNOWLEDGMENTS

REFERENCES

[1] H. Huang and K. Kim, PRSTAB, Volume 5, 074401 and 129903 (2002).

[2] H. Huang, M. Borland, P. Emma and K. Kim, NIMA, 507 (2003), 318-322.

[3] S. Heifets, G. Stupakov and S. Krinsky, PRSTAB, Volume 5, 064401 (2002).

[4] M. Borland, PRSTAB, Volume 11, 030701, (2008).

[5] M. Venturini, R. Warnock and A. Zholents, PRSTAB, Volume 10, 054403, (2007).

[6] M. Venturini, PRSTAB, Volume 10, 104401, (2007).

[7] J. A. Ellison, G. Bassi, K. Heinemann, M. Venturini and R. Warnock, Proceedings of PAC2007, Albuquerque, USA.

[8] G. Bassi, J. A. Ellison, K. Heinemann and R. Warnock, Proceedings of PAC2007, Albuquerque, USA.

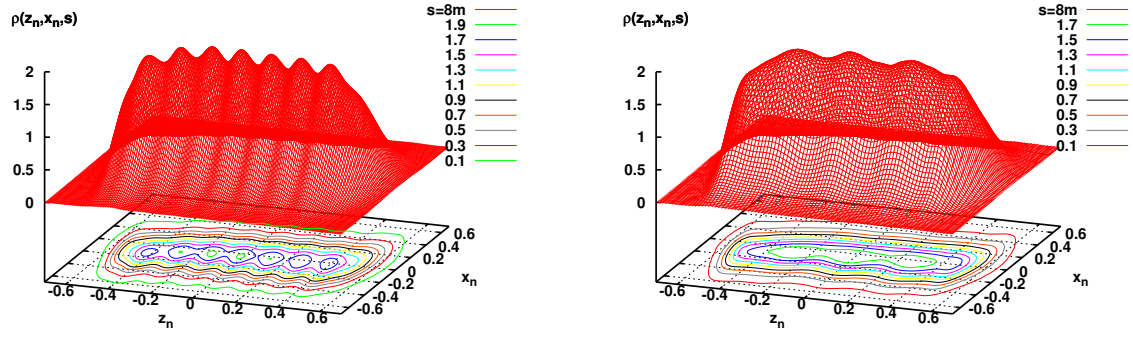[9] R. Warnock, J. A. Ellison, K. Heinemann, G.Q. Zhang, These Proceedings, Paper TUPP109.

Figure 3: Charge density in normalized coordinates at s=8m for $\lambda = 300\mu$m (left frame) and $\lambda = 600\mu$m (right frame).
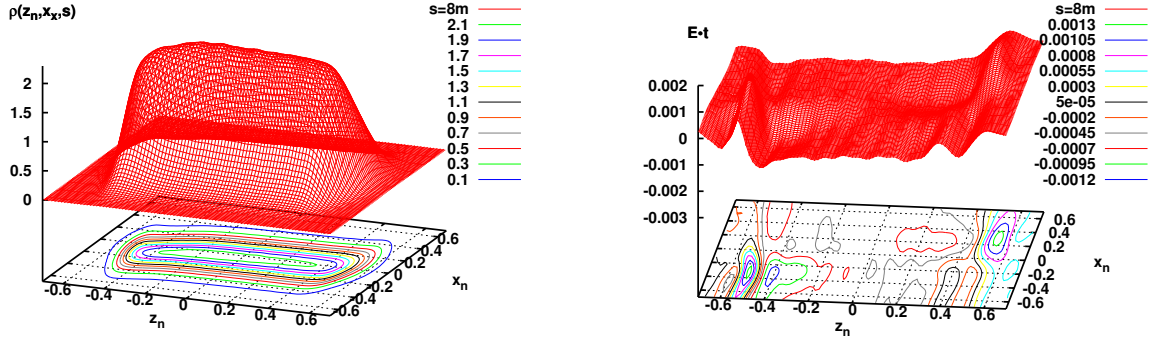

Figure 4: Left frame: charge density in normalized coordinates at s=8m with no initial modulation. Right frame: longitudinal component of the electric field $\mathbf{E} \cdot \mathbf{t}$ in normalized coordinates at s=8m with no initial modulation.
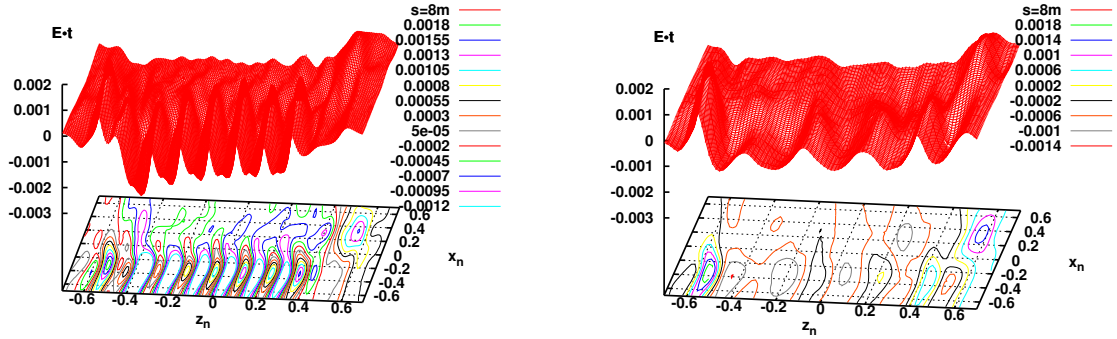

Figure 5: Longitudinal component of the electric field $\mathbf{E} \cdot \mathbf{t}$ in normalized coordinates at s=8m for $\lambda = 300\mu$m (left frame) and $\lambda = 600\mu$m (right frame).